

## Accepted Manuscript

Synthesis and biological evaluation of CHX-DAPYs as HIV-1 non-nucleoside reverse transcriptase inhibitors

Zi-Hong Yan, Hai-Qiu Wu, Wen-Xue Chen, Yan Wu, Hu-Ri Piao, Qiu-Qin He, Fen-Er Chen, Erik De Clercq, Christophe Pannecouque

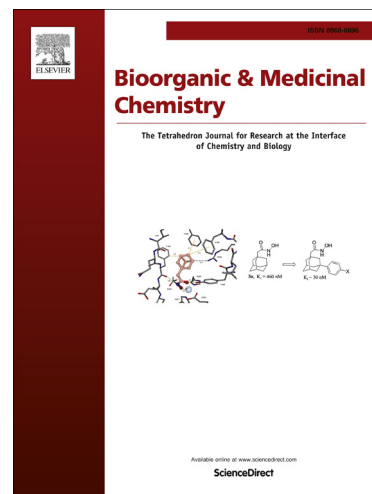
PII: S0968-0896(14)00193-X  
DOI: <http://dx.doi.org/10.1016/j.bmc.2014.03.020>  
Reference: BMC 11467

To appear in: *Bioorganic & Medicinal Chemistry*

Received Date: 12 February 2014  
Revised Date: 8 March 2014  
Accepted Date: 11 March 2014

Please cite this article as: Yan, Z-H., Wu, H-Q., Chen, W-X., Wu, Y., Piao, H-R., He, Q-Q., Chen, F-E., De Clercq, E., Pannecouque, C., Synthesis and biological evaluation of CHX-DAPYs as HIV-1 non-nucleoside reverse transcriptase inhibitors, *Bioorganic & Medicinal Chemistry* (2014), doi: <http://dx.doi.org/10.1016/j.bmc.2014.03.020>

This is a PDF file of an unedited manuscript that has been accepted for publication. As a service to our customers we are providing this early version of the manuscript. The manuscript will undergo copyediting, typesetting, and review of the resulting proof before it is published in its final form. Please note that during the production process errors may be discovered which could affect the content, and all legal disclaimers that apply to the journal pertain.



**Graphical Abstract**

To create your abstract, type over the instructions in the template box below.  
 Fonts or abstract dimensions should not be changed or altered.

**Synthesis and biological evaluation of CHX-DAPYs as HIV-1 non-nucleoside reverse transcriptase inhibitors**

Leave this area blank for abstract info.

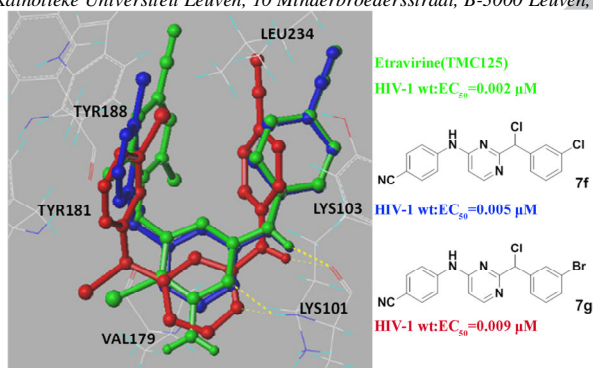
Zi-Hong Yan<sup>a</sup>, Hai-Qiu Wu<sup>a</sup>, Wen-Xue Chen<sup>a</sup>, Yan Wu<sup>b</sup>, Hu-Ri Piao<sup>b</sup>, Qiu-Qin He<sup>a,\*</sup>, Fen-Er Chen<sup>a,c,\*</sup>, Erik De Clercq<sup>d</sup>, and Christophe Pannecouque<sup>d</sup>

<sup>a</sup> Department of Chemistry, Fudan University, Shanghai 200433, People's Republic of China

<sup>b</sup> College of Pharmacy, Yanbian University, Yanji 133000, People's Republic of China

<sup>c</sup> Institute of Biomedical Science, Fudan University, Shanghai 200433, People's Republic of China

<sup>d</sup> Rega Institute for Medical Research, Katholieke Universiteit Leuven, 10 Minderbroedersstraat, B-3000 Leuven, Belgium





## Synthesis and biological evaluation of CHX-DAPYs as HIV-1 non-nucleoside reverse transcriptase inhibitors

 Zi-Hong Yan<sup>a</sup>, Hai-Qiu Wu<sup>a</sup>, Wen-Xue Chen<sup>a</sup>, Yan Wu<sup>b</sup>, Hu-Ri Piao<sup>b</sup>, Qiu-Qin He<sup>a,\*</sup>, Fen-Er Chen<sup>a,c,\*</sup>, Erik De Clercq<sup>d</sup>, and Christophe Pannecouque<sup>d</sup>
<sup>a</sup> Department of Chemistry, Fudan University, Shanghai 200433, People's Republic of China

<sup>b</sup> College of Pharmacy, Yanbian University, Yanji 133000, People's Republic of China

<sup>c</sup> Institute of Biomedical Science, Fudan University, Shanghai 200433, People's Republic of China

<sup>d</sup> Rega Institute for Medical Research, Katholieke Universiteit Leuven, 10 Minderbroedersstraat, B-3000 Leuven, Belgium

## ARTICLE INFO

## ABSTRACT

## Article history:

Received

Received in revised form

Accepted

Available online

## Keywords:

HIV-1

NNRTIs

diarylpyrimidine

SAR

Antiviral activity

A series of new diarylpyrimidines (DAPYs) characterized by a halogen atom on the methylene linker between wing I and the central pyrimidine ring was synthesized and evaluated for their anti-HIV activity in MT-4 cell cultures. The two most promising compounds **7f** and **7g** showed excellent activity against wild-type HIV-1 with low nanomolar EC<sub>50</sub> values of 0.005 μM and 0.009 μM, respectively, which were comparable to or more potent than all the reference drugs zidovudine (AZT), lamivudine (3TC), nevirapine (NEV), efavirenz (EFV), delavirdine (DLV) and etravirine (ETV). In particular, **7g** also displayed strong activity against the double mutant strain 103N+181C with an EC<sub>50</sub> value of 8.2 μM. The preliminary structure–activity relationship (SAR) and molecular docking analysis of this new series of CHX-DAPYs were also investigated.

2009 Elsevier Ltd. All rights reserved.

## 1. Introduction

The reverse transcriptase of human immunodeficiency virus type 1 (HIV-1 RT) is an essential enzyme for viral replication and represents one of the main targets for antiretroviral chemotherapy.<sup>1</sup> The inhibitors of this enzyme can be divided into two broad classes: nucleoside/nucleotide reverse transcriptase inhibitors (NRTIs) and non-nucleoside reverse transcriptase inhibitors (NNRTIs). NRTIs inhibit viral replication by binding directly to the polymerase active site, whereas NNRTIs specifically bind to an allosteric hydrophobic site, called the non-nucleoside reverse transcriptase inhibitor binding pocket (NNIBP), which lies approximately 10 Å away from the active site.<sup>2,3</sup> As indispensable components in highly active antiretroviral therapy (HAART), NNRTIs have gained a definitive and important place in clinical use. NNRTIs currently approved for AIDS therapy include nevirapine (NVP, **1**, Figure 1), delavirdine (DLV, **2**, Figure 1), efavirenz (EFV, **3**, Figure 1), etravirine (TMC125, ETV, **4**, Figure 1) and rilpivirine (TMC278, **5**, Figure 1). Among numerous efforts to develop structurally different NNRTIs, the diarylpyrimidine derivatives (DAPYs) represented by etravirine and rilpivirine have been

regarded as one of the most successful scaffolds for structural modification to obtain more promising anti-HIV agents due to their excellent potency and low cytotoxicity.<sup>4-9</sup>

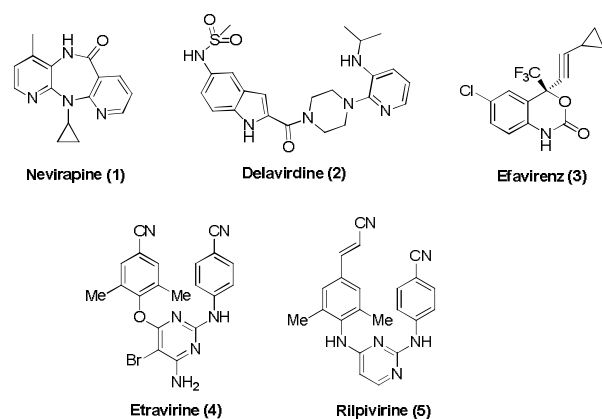
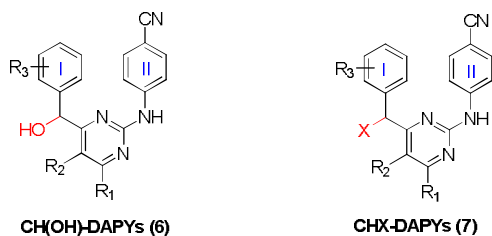


Figure 1. Structures of currently FDA-approved clinical NNRTIs.

\* Corresponding author. Tel.: +86 21 65643809; fax: +86 21 65643811; e-mail: qqhe@fudan.edu.cn

\* Corresponding author. Tel.: +86 21 65643809; fax: +86 21 65643811; e-mail: rfchen@fudan.edu.cn

In our previous DAPY project, we focused on structural modification of the linker between wing I and the central pyrimidine ring and identified CH(OH)-DAPYs (**6**, **Figure 2**) as a new class of potent NNRTIs.<sup>10</sup> Among these CH(OH)-DAPYs, the most potent compound **6a** ( $R_1 = R_2 = H$ ,  $R_3 = 2\text{-Cl}$ ) displayed anti-HIV-1 activity with an  $EC_{50}$  value of 0.009  $\mu\text{M}$ . It indicates that introduction of a small group at the  $\text{CH}_2$  linker is tolerable for antiviral activity. On the basis of this result and hydrophobic property of NNIBP, a halogen atom was introduced to  $\text{CH}_2$  linker with the aim to enhance the ligand-protein binding affinity via hydrophobic interaction between the added halogen atom and NNIBP. Thus we report herein the design, synthesis, and anti-HIV activity of these CHX-DAPYs (**7**, **Figure 2**).



**Figure 2.** Structures of CH(OH)-DAPYs and CHX-DAPYs.

## 2. Chemistry

The synthetic route to the target compounds **7a-s** is depicted in **Scheme 1**. The key intermediates 4-((4-(hydroxy(phenyl)methyl)pyrimidin-2-yl)amino)benzonitrile **14a-q** were prepared from **8a-c** according to our previously reported protocol in 6 steps.<sup>10</sup> Halogenation of **14a-q** with thionyl chloride or phosphorus tribromide in anhydrous dichloromethane afforded the target compounds **7a-s** in 45-78% yields.

## 3. Results and discussion

### 3.1. Biological activity

The newly synthesized compounds **7a-s** were tested in infected MT-4 cells to evaluate their antiviral activity against wild-type HIV-1 (LAI strain IIIB), double mutant HIV-1 strain RES056 (K103N + Y181C) and HIV-2 strain ROD. AZT, 3TC, NVP, EFV, DLV and ETV were used as reference drugs in the test. The results, expressed as  $EC_{50}$  (anti-HIV activity),  $CC_{50}$  (cytotoxicity) and SI (selectivity index, given by the  $CC_{50}/EC_{50}$  ratio), are summarized in **Table 1**.

As shown in **Table 1**, all the compounds **7a-s** showed moderate to excellent inhibitory activity against wild-type HIV-1 with  $EC_{50}$  values ranging from 7.880 to 0.005  $\mu\text{M}$ . The two most potent compounds **7f** and **7g** had low nanomolar  $EC_{50}$  values of 0.005  $\mu\text{M}$  and 0.009  $\mu\text{M}$ , respectively, which were comparable to or more active than all the reference drugs AZT, 3TC, NVP, EFV, DLV and ETV. SI values of both **7f** and **7g** were  $>3000$ . In particular, **7g** also strongly inhibited the double mutant strain 103N+181C with an  $EC_{50}$  value of 8.2  $\mu\text{M}$ . None of the tested NNRTIs including the newly synthesized CHX-DAPYs and the reference drugs NVP, EFV, DLV, ETV showed activity against HIV-2 strain ROD.

To explore SAR of this new series of CHX-DAPYs, the modifications are focused on  $\text{CH}_2$  linker, the central pyrimidine ring as well as the wing I. First we examined the effect of introducing different halogen atom into  $\text{CH}_2$  linker between wing I and the central pyrimidine ring. The biological results showed that **7a** ( $X = \text{Cl}$ ,  $EC_{50} = 0.016 \mu\text{M}$ ) displayed approximately 10-fold stronger antiviral activity than **7r** ( $X = \text{Br}$ ,  $EC_{50} = 0.200 \mu\text{M}$ ).

Interestingly, the introduction of a methyl group at the *para* position of the benzene ring of **7a** resulted into **7b** ( $EC_{50} = 0.069 \mu\text{M}$ ), which appeared to be slightly less active than the corresponding **7s** ( $EC_{50} = 0.047 \mu\text{M}$ ).

Next we examined the effect of introducing substituents into the central pyrimidine ring. Compound **7d** ( $X = \text{Cl}$ ,  $R_1 = R_2 = H$ ,  $R_3 = 4\text{-}t\text{-butyl-phenyl}$ ) was as potent as **7i** ( $X = \text{Cl}$ ,  $R_1 = \text{Me}$ ,  $R_2 = H$ ,  $R_3 = 4\text{-}t\text{-butyl-phenyl}$ ), but 10-fold more potent than **7o** ( $X = \text{Cl}$ ,  $R_1 = H$ ,  $R_2 = \text{Me}$ ,  $R_3 = 4\text{-}t\text{-butyl-phenyl}$ ). As consistent with the results obtained previously on the CHOH-DAPYs, compound **7h** ( $X = \text{Cl}$ ,  $R_1 = R_2 = H$ ,  $R_3 = 4\text{-F-phenyl}$ ) showed higher activity than that of **7m** ( $X = \text{Cl}$ ,  $R_1 = \text{Me}$ ,  $R_2 = H$ ,  $R_3 = 4\text{-F-phenyl}$ ) and **7p** ( $X = \text{Cl}$ ,  $R_1 = H$ ,  $R_2 = \text{Me}$ ,  $R_3 = 4\text{-F-phenyl}$ ), compound **7j** ( $X = \text{Cl}$ ,  $R_1 = R_2 = H$ ,  $R_3 = 4\text{-Br-phenyl}$ ) was more potent than **7n** ( $X = \text{Cl}$ ,  $R_1 = \text{Me}$ ,  $R_2 = H$ ,  $R_3 = 4\text{-Br-phenyl}$ ) and **7q** ( $X = \text{Cl}$ ,  $R_1 = H$ ,  $R_2 = \text{Me}$ ,  $R_3 = 4\text{-Br-phenyl}$ ). These results suggested that no substituent at pyrimidine ring may be favorable for antiviral potency.

Finally we examined the effect of introducing substituents into the benzene ring of wing I. The introduction of a methyl, methoxy or *tert*-butyl group at the *para* position of **7a** led to significantly decreased activity against wild-type HIV-1. The introduction of a halogen group at the *meta* or *para* position of **7a** led to compounds **7e-j**, whose inhibitory activity seemed to be greatly influenced by the position of the introduced halogen group. Compounds **7e-g** with a halogen atom at *meta* position of **7a** were more active than the corresponding *para*-position halogenated compounds **7h-j**. Moreover, chlorinated or brominated compounds exhibited significantly stronger potency than the corresponding fluorinated derivatives. For example, **7f** (3-Cl) and **7g** (3-Br) were more active than **7e** (3-F). Similarly, **7i** (4-Cl) and **7j** (4-Br) were more potent than **7h** (4-F). The replacement of benzene ring of **7a** with a bulky naphthyl group led to **7k**, which showed decreased antiviral activity.

### 3.2. Molecular modeling analysis

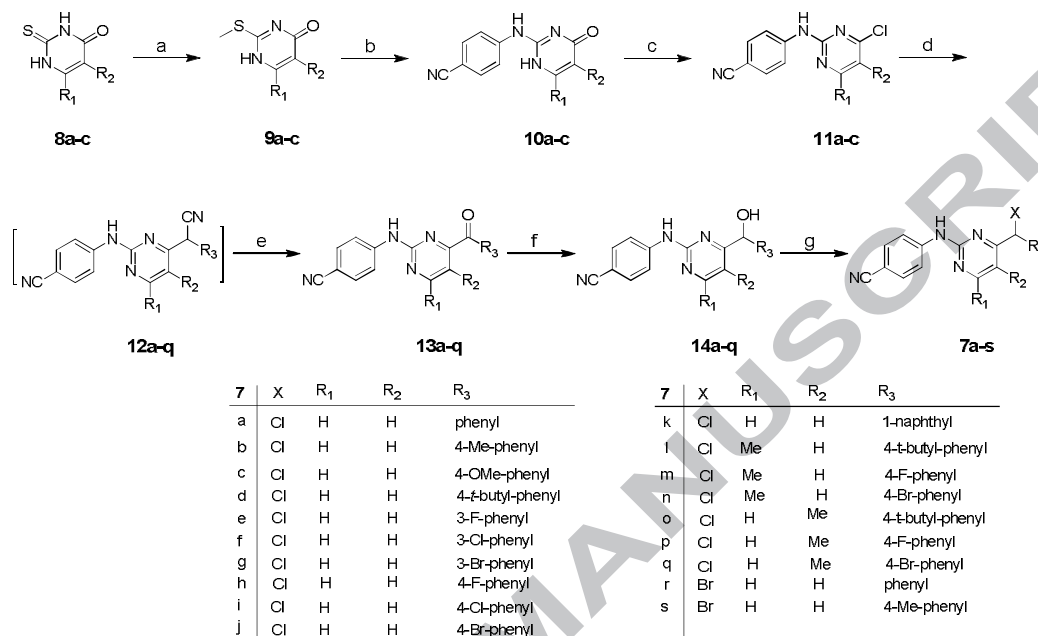
With the aim to investigate the binding mode of CHX-DAPYs in NNIBP of wild-type HIV-1 RT, molecular docking was performed using Sybyl Surflex-Dock program. The crystal structure of RT in complex with ETV (PDB ID: 3MEC) was used for molecular docking and the representative compounds **7f** and **7g** were chosen for docking analysis. Compound **7f** was the most active one tested against wild-type HIV-1 among the newly synthesized compounds, while **7g** was the only one endowed with inhibitory activity against double mutant strain 103N+181C.

As shown in **Figure 3a**, both representative compounds adopted very similar binding orientations and horseshoe conformational shapes in NNIBP to that of ETV. Two typical hydrogen bonds were clearly observed with all three compounds, which are crucial for antiviral activity of DAPYs. One hydrogen bond was between N-1 of pyrimidine ring and  $\text{NH}_2$  group of the residue Lys101, another involved the NH linker and C=O group of Lys101. The wing I of both **7f** and **7g** provided strong  $\pi$ -stacking interaction with the residues Tyr181 and Tyr188. However, the orientation of **7f** moved downward compared to those of **7g** and ETV and no interaction with the residues Phe227 and Trp229 could be observed. This may determine the loss of the inhibitory activity for **7f** against mutant virus.

From **Figures 3b** and **3c**, it is important to note that the chloride atom of the linker for **7f** could form halogen bond with C=O group of Tyr188 ( $d \text{O} \cdots \text{Cl} = 2.67 \text{ \AA}$ ; angle  $\text{O} \cdots \text{Cl} \cdots \text{C} \approx 140^\circ$ ), whereas **7g** could not exhibit this halogen bond ( $d \text{O} \cdots \text{Cl} = 5.94 \text{ \AA}$ ).<sup>11-16</sup> It may explain why **7f** displayed higher anti-HIV-1 activity than **7g**.

To further explore the interaction of CHX-DAPYs with mutated HIV-1 RT, compounds **7f** and **7g** were also docked into NNIBP of mutant HIV-1 RT (K103N/Y181C) in complex with TMC278 (PDB ID: 3BGR). As illustrated in **Figure 4**, **7g** is predicted to bind with NNIBP still in a horseshoe conformational shape similar to that of TMC278 and it kept the two typical hydrogen bonds with Lys101; however, **7f** bound with NNIBP in a totally different mode from **7g** and TMC278. The orientation of

the horseshoe shape for **7f** was downward and no direct interactions between **7f** and binding site could be observed. This might reveal the reason why compound **7g** could inhibit the replication of double mutant strain 103N+181C, whereas **7f** was completely inactive, although these two compounds differ structurally only in the identity of the substituents on the benzene ring of wing I.



**Scheme 1.** Synthetic route to compounds **7a-s**. Reagents and conditions: a) MeI, NaOH, H<sub>2</sub>O, rt, 24 h; b) 4-cyanoaniline, 180-190 °C, 8 h; c) POCl<sub>3</sub>, reflux, 0.5 h; d) substituted phenylacetonitrile, 60% NaH, Ar, DMF, -20 °C to rt, 48-72 h; e) air, rt, 48-72 h; f) KBH<sub>4</sub>, methanol, -20 °C to rt, 2 h; g) SOCl<sub>2</sub> or PBr<sub>3</sub>, dichloromethane.

**Table 1.** Anti-HIV-1 activities and cytotoxicity of compounds **7a-s** in MT-4 cells<sup>a</sup>

compd	EC <sub>50</sub> [μM] <sup>b</sup>			CC <sub>50</sub> [μM] <sup>c</sup>	SI <sup>d</sup> WT(III <sub>B</sub> )
	WT(III <sub>B</sub> )	K103N+Y181C	HIV-2		
<b>7a</b>	0.016±0.003	>37.8	>37.8	37.8	2336
<b>7b</b>	0.069±0.006	>49.7	>49.7	49.7	713
<b>7c</b>	0.219±0.022	>33.6	>33.6	≥33.6	154
<b>7d</b>	0.170±0.092	>32.9	>32.9	32.9	193
<b>7e</b>	1.358±0.472	>36.8	>36.8	36.8	27
<b>7f</b>	0.005±0.003	>24.3	>24.3	24.3	5162
<b>7g</b>	0.009±0.001	8.2±0.05	>30.4	30.4	3106
<b>7h</b>	1.830±0.177	>35.4	>35.4	35.4	19
<b>7i</b>	0.068±0.014	>36.1	>36.1	36.1	545
<b>7j</b>	0.038±0.013	>32.5	>32.5	32.5	875
<b>7k</b>	0.202±0.024	>11.3	>11.3	11.3	56
<b>7l</b>	0.174±0.070	>30.3	>30.3	30.3	173
<b>7m</b>	5.839±1.729	>31.1	>31.1	31.1	5
<b>7n</b>	0.435±0.230	>31.9	>31.9	31.9	75
<b>7o</b>	1.791±0.716	>28.7	>28.7	28.7	16
<b>7p</b>	7.880±2.154	>30.8	>30.8	30.8	4
<b>7q</b>	0.109±0.073	>10.3	>10.3	10.3	95
<b>7r</b>	0.200±0.088	>69.0	>69.0	69.0	348
<b>7s</b>	0.047±0.011	>31.5	>31.5	31.5	672
AZT	0.006±0.001	0.007±0.001	0.005±0.000	>93.5	>17045

3TC	2.442±0.262	ND <sup>a</sup>	7.2±0.8	>87.2	>36
NVP	0.090±0.015	>15.0	ND <sup>c</sup>	15.0	>163
EFV	0.006±0.001	0.270±0.108	ND <sup>c</sup>	>6.3	>1136
DLV	0.085±0.007	>43.8	ND <sup>c</sup>	>43.8	>511
ETV	0.002±0.0005	0.0147	>14.25	14.25	7383

<sup>a</sup> Data represent the mean of at least three separate experiments.

<sup>b</sup> Compound concentration required to inhibit MT-4 cells against viral cytopathogenicity by 50%.

<sup>c</sup> Compound concentration that decreases the uninfected MT-4 cell viability by 50%.

<sup>d</sup> Selectivity index: CC<sub>50</sub>/IC<sub>50</sub> ratio.

<sup>e</sup> Not detected.

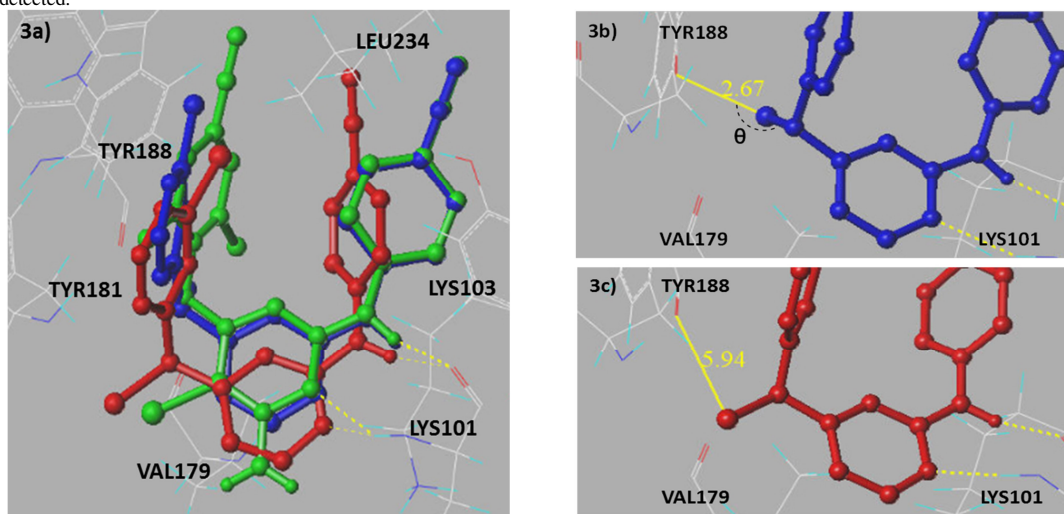


**Fig. 3.** Predicted binding mode of the representative compounds in NNIBP of wild type HIV-1 RT (PDB ID: 3MEC): a) compound **7f** (blue) and **7g** (red), **ETV** (green) was superposed into the same pocket for comparison, b) halogen bond of compound **7f** (blue), c) halogen bond of compound **7g** (red). Possible hydrogen bonds between the inhibitors and the residues are indicated with dashed lines (yellow).

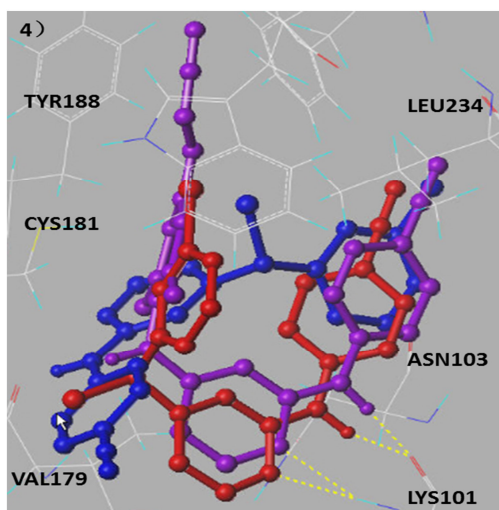


**Fig. 4.** Predicted binding mode of the representative compounds in NNIBP of double mutant (K103N/Y181C) (PDB code: 3BGR), compound **7f** (blue) and **7g** (red), **TMC278** (purple) was superposed into the same pocket for comparison.

#### 4. Conclusion

In conclusion, a new series of new CHX-DAPYs featuring a halogen atom at CH<sub>2</sub> linker between wing I and the central pyrimidine ring was synthesized and evaluated against wild-type HIV-1, HIV-2 and drug-resistant viral strain in cellular assays. All the target compounds displayed anti-HIV-1 activity with micromolar to nanomolar EC<sub>50</sub> values in infected MT-4 cells. Compounds **7f** and **7g** exhibited the most antiviral activity with

EC<sub>50</sub> values of 0.005 μM and 0.009 μM, respectively, which were comparable to or more active than all the six reference drugs AZT, 3TC, NVP, EFV, DLV and ETV. Moreover, **7g** was also active against the double mutant strain 103N+181C. The binding modes with wide-type HIV-1 RT suggested that the added halogen atom at CH<sub>2</sub> linker for **7f** could form halogen bond with C=O group of Tyr188 and thus enhanced its binding affinity resulting in an improved antiviral activity. The binding modes with mutant HIV-1 RT showed that **7g** still adopted a horseshoe conformational shape in NNIBP and kept two hydrogen bonds with Lys101; this may be the reason why **7g** could remain the activity against drug-resistant viral strain.

#### 5. Material and methods

##### 5.1. Chemistry

Melting points were measured on a SGW X-1 microscopic melting-point apparatus. <sup>1</sup>H NMR and <sup>13</sup>C NMR spectra on a Bruker AV 400 MHz spectrometer were recorded in DMSO-*d*<sub>6</sub>. Chemical shifts are reported in δ (ppm) units relative to the internal standard tetramethylsilane (TMS). Mass spectra were obtained on a Waters Quattro Micromass instrument using electrospray ionization (ESI) techniques. Infrared spectra (IR) were recorded with a nexus FT/IR-4200 spectro-meter. All chemicals and solvents used were of reagent grade and were purified and dried by standard methods before use. All air-sensitive reactions were run under a nitrogen atmosphere. All the reactions were monitored by thin layer chromatography (TLC) on pre-coated silica gel G plates at 254 nm under a UV lamp using ethyl acetate/petroleum ether as eluent. Flash chromatography separations were obtained on silica gel (300–400 mesh). All yields are unoptimized and only represent one experiment's result.

## 5.2. General procedure for preparation of target compounds 7a-q

To a solution of **14a-q** (1 mmol) in anhydrous dichloromethane (10 mL) was added thionyl chloride (1.0 mL) dropwise at  $-20\text{ }^{\circ}\text{C}$ . After being stirred for 2 h at room temperature, the mixture was poured into ice water (20 mL) and extracted with ethyl acetate (3 $\times$ 20 mL). The combined organic layers were washed with 5% aqueous sodium hydrogen carbonate and brine, dried over anhydrous sodium sulfate, and concentrated in vacuo. The residue was purified by column chromatography on silica gel (ethyl acetate/hexane, 1: 2) to give the desired compounds.

## 5.3. General procedure for preparation of target compounds 7r-s

To a solution of **14a-b** (1 mmol) in anhydrous dichloromethane (10 mL) was added phosphorus tribromide (1.35 g, 5 mmol). After being stirred for 1.5 h at room temperature, the mixture was poured into ice water (20 mL) and extracted with ethyl acetate (3 $\times$ 20 mL). The combined organic layers were washed with 5% aqueous sodium hydrogen carbonate and brine, dried over anhydrous sodium sulfate, and concentrated in vacuo. The residue was purified by column chromatography on silica gel (ethyl acetate/hexane, 1: 2) to give the desired compounds **7r-s**.

### 5.2.1. 4-((4-(chloro(phenyl)methyl)pyrimidin-2-yl)amino)benzotrile (7a).

Yield 51%; light yellow solid; mp 145.0-145.4 $^{\circ}\text{C}$ ;  $^1\text{H}$  NMR (400MHz, DMSO- $d_6$ )  $\delta$  (ppm) 6.37 (s, 1 H, CH), 7.19 (d,  $J = 5.2$  Hz, 1 H, pyrimidine  $H_5$ ), 7.35-7.40 (m, 1 H,  $\text{ArH}_4$ ), 7.43 (d,  $J = 7.6$  Hz, 2 H,  $\text{ArH}_{3,5}$ ), 7.55 (d,  $J = 8.4$  Hz, 2 H,  $\text{ArH}_{2,6}$ ), 7.69 (d,  $J = 8.8$  Hz, 2 H,  $\text{ArH}_{2,6}$ ), 7.91 (d,  $J = 8.8$  Hz, 2 H,  $\text{ArH}_{3,5}$ ), 8.62 (d,  $J = 5.2$  Hz, 1 H, pyrimidine  $H_6$ ), 10.31 (s, 1 H, NH);  $^{13}\text{C}$  NMR (100MHz, DMSO- $d_6$ )  $\delta$  (ppm) 62.23, 102.67, 111.12, 118.46, 128.12, 128.71, 128.75, 132.97, 138.94, 144.65, 159.17, 159.85, 167.87; IR (KBr,  $\text{cm}^{-1}$ ) 2220 (CN); MS (ESI)  $m/z$  321 [M+H] $^{+}$ .

### 5.2.2. 4-((4-(chloro(p-tolyl)methyl)pyrimidin-2-yl)amino)benzotrile (7b).

Yield 66%; yellow solid; mp 127.0-127.8 $^{\circ}\text{C}$ ;  $^1\text{H}$  NMR (400MHz, DMSO- $d_6$ )  $\delta$  (ppm) 2.28 (s, 3 H, Me), 6.32 (s, 1 H, CH), 7.16 (d,  $J = 5.2$  Hz, 1 H, pyrimidine  $H_5$ ), 7.21 (d,  $J = 7.6$  Hz, 2 H,  $\text{ArH}_{3,5}$ ), 7.43 (d,  $J = 8.0$  Hz, 2 H,  $\text{ArH}_{2,6}$ ), 7.69 (d,  $J = 8.8$  Hz, 2 H,  $\text{ArH}_{2,6}$ ), 7.94 (d,  $J = 8.8$  Hz, 2 H,  $\text{ArH}_{3,5}$ ), 8.61 (d,  $J = 4.8$  Hz, 1 H, pyrimidine  $H_6$ ), 10.32 (s, 1 H, NH);  $^{13}\text{C}$  NMR (100MHz, DMSO- $d_6$ )  $\delta$  (ppm) 20.73, 62.27, 102.65, 111.02, 118.46, 128.02, 129.25, 132.93, 132.97, 136.01, 138.19, 144.67, 159.16, 159.76, 167.99; IR (KBr,  $\text{cm}^{-1}$ ) 2219 (CN); MS (ESI)  $m/z$  335 [M+H] $^{+}$ .

### 5.2.3. 4-((4-(chloro(4-methoxyphenyl)methyl)pyrimidin-2-yl)amino)benzotrile (7c).

Yield 58%; yellow solid; mp 177.7-178.2 $^{\circ}\text{C}$ ;  $^1\text{H}$  NMR (400MHz, DMSO- $d_6$ )  $\delta$  (ppm) 3.73 (s, 3 H, OMe), 6.30 (s, 1 H, CH), 6.95 (d,  $J = 8.4$  Hz, 2 H,  $\text{ArH}_{3,5}$ ), 7.15 (d,  $J = 5.2$  Hz, 1 H, pyrimidine  $H_5$ ), 7.47 (d,  $J = 8.4$  Hz, 2 H,  $\text{ArH}_{2,6}$ ), 7.69 (d,  $J = 8.4$  Hz, 2 H,  $\text{ArH}_{2,6}$ ), 7.97 (d,  $J = 8.8$  Hz, 2 H,  $\text{ArH}_{3,5}$ ), 8.60 (d,  $J = 5.2$  Hz, 1 H, pyrimidine  $H_6$ ), 10.31 (s, 1 H, NH);  $^{13}\text{C}$  NMR (100MHz, DMSO- $d_6$ )  $\delta$  (ppm) 55.20, 62.29, 102.69, 110.92, 114.07, 118.48, 129.51, 130.90, 132.92, 144.68, 159.17, 159.44, 159.65, 168.05; IR (KBr,  $\text{cm}^{-1}$ ): 2221 (CN); MS (ESI)  $m/z$  349 [M-H] $^{-}$ .

### 5.2.4. 4-((4-(4-(tert-butyl)phenyl)chloromethyl)pyrimidin-2-yl)amino)benzotrile (7d).

Yield 63%; light yellow solid; mp 143.5-144.0 $^{\circ}\text{C}$ ;  $^1\text{H}$  NMR (400MHz, DMSO- $d_6$ )  $\delta$  (ppm) 1.24 (s, 9 H, *t*-butyl), 6.32 (s, 1 H, CH), 7.18 (d,  $J = 5.2$  Hz, 1 H, pyrimidine  $H_5$ ), 7.41 (d,  $J = 8.4$  Hz, 2 H,  $\text{ArH}_{3,5}$ ), 7.47 (d,  $J = 8.4$  Hz, 2 H,  $\text{ArH}_{2,6}$ ), 7.69 (d,  $J = 8.8$  Hz, 2 H,  $\text{ArH}_{2,6}$ ), 7.95 (d,  $J = 8.8$  Hz, 2 H,  $\text{ArH}_{3,5}$ ), 8.61 (d,  $J = 4.8$  Hz, 1 H, pyrimidine  $H_6$ ), 10.31 (s, 1 H, NH);  $^{13}\text{C}$  NMR (100MHz, DMSO- $d_6$ )  $\delta$  (ppm) 30.97, 34.34, 62.16, 102.63, 110.99, 118.45, 125.49, 127.79, 132.92, 135.96, 144.64, 151.20, 159.15, 159.73, 167.92; IR (KBr,  $\text{cm}^{-1}$ ) 2219 (CN); MS (ESI)  $m/z$  377 [M+H] $^{+}$ .

### 5.2.5. 4-((4-(chloro(3-fluorophenyl)methyl)pyrimidin-2-yl)amino)benzotrile (7e).

Yield 59%; yellow solid; mp 109.6-110.5 $^{\circ}\text{C}$ ;  $^1\text{H}$  NMR (400MHz, DMSO- $d_6$ )  $\delta$  (ppm) 6.43 (s, 1 H, CH), 7.19 (d,  $J = 4.8$  Hz, 1 H, pyrimidine  $H_5$ ), 7.23 (s, 1 H,  $\text{ArH}_2$ ), 7.39-7.43 (m, 2 H,  $\text{ArH}_{4,6}$ ), 7.45-7.50 (m, 1 H,  $\text{ArH}_5$ ), 7.68 (d,  $J = 8.4$  Hz, 2 H,  $\text{ArH}_{2,6}$ ), 7.91 (d,  $J = 8.4$  Hz, 2 H,  $\text{ArH}_{3,5}$ ), 8.63 (d,  $J = 4.8$  Hz, 1 H, pyrimidine  $H_6$ ), 10.33 (s, 1 H, NH);  $^{13}\text{C}$  NMR (100MHz, DMSO- $d_6$ )  $\delta$  (ppm) 61.07, 102.73, 111.16, 114.89, 115.11, 115.73, 118.46, 124.27, 124.30, 130.76, 130.84, 132.91, 144.58, 159.18, 159.98, 167.26; IR (KBr,  $\text{cm}^{-1}$ ) 2220 (CN); MS (ESI)  $m/z$  337 [M-H] $^{-}$ .

### 5.2.6. 4-((4-(chloro(3-chlorophenyl)methyl)pyrimidin-2-yl)amino)benzotrile (7f).

Yield 68%; light yellow solid; mp 130.1-130.6 $^{\circ}\text{C}$ ;  $^1\text{H}$  NMR (400MHz, DMSO- $d_6$ )  $\delta$  (ppm) 6.43 (s, 1 H, CH), 7.19 (d,  $J = 4.8$  Hz, 1 H, pyrimidine  $H_5$ ), 7.24 (s, 1 H,  $\text{ArH}_2$ ), 7.39-7.43 (m, 2 H,  $\text{ArH}_{4,6}$ ), 7.45-7.50 (m, 1 H,  $\text{ArH}_5$ ), 7.68 (d,  $J = 8.4$  Hz, 2 H,  $\text{ArH}_{2,6}$ ), 7.91 (d,  $J = 8.4$  Hz, 2 H,  $\text{ArH}_{3,5}$ ), 8.63 (d,  $J = 4.8$  Hz, 1 H, pyrimidine  $H_6$ ), 10.33 (s, 1 H, NH);  $^{13}\text{C}$  NMR (100MHz, DMSO- $d_6$ )  $\delta$  (ppm) 61.07, 102.73, 111.16, 114.89, 115.11, 115.73, 118.46, 124.27, 124.30, 130.76, 130.84, 132.91, 144.58, 159.18, 159.98, 167.26; IR (KBr,  $\text{cm}^{-1}$ ) 2218 (CN); MS (ESI)  $m/z$  354 [M-H] $^{-}$ .

### 5.2.7. 4-((4-(3-bromophenyl)chloromethyl)pyrimidin-2-yl)amino)benzotrile (7g).

Yield 78%; light yellow solid; mp 140.1-140.6 $^{\circ}\text{C}$ ;  $^1\text{H}$  NMR (400MHz, DMSO- $d_6$ )  $\delta$  (ppm) 6.42 (s, 1 H, CH), 7.21 (d,  $J = 5.2$  Hz, 1 H, pyrimidine  $H_5$ ), 7.37-7.41 (m, 1 H,  $\text{ArH}_5$ ), 7.55-7.59 (m, 2 H,  $\text{ArH}_{4,6}$ ), 7.69 (d,  $J = 8.8$  Hz, 2 H,  $\text{ArH}_{2,6}$ ), 7.68 (s, 1 H,  $\text{ArH}_2$ ), 7.89 (d,  $J = 8.8$  Hz, 2 H,  $\text{ArH}_{3,5}$ ), 8.63 (d,  $J = 4.8$  Hz, 1 H, pyrimidine  $H_6$ ), 10.33 (s, 1 H, NH);  $^{13}\text{C}$  NMR (100MHz, DMSO- $d_6$ )  $\delta$  (ppm) 60.92, 102.73, 111.15, 118.46, 121.70, 127.21, 130.79, 130.95, 131.57, 132.93, 141.41, 144.56, 58, 159.18, 160.05, 167.19; IR (KBr,  $\text{cm}^{-1}$ ) 2221 (CN); MS (ESI)  $m/z$  399 [M+H] $^{+}$ .

### 5.2.8. 4-((4-(chloro(4-fluorophenyl)methyl)pyrimidin-2-yl)amino)benzotrile (7h).

Yield 62%; light yellow solid; mp 161.2-162.0 $^{\circ}\text{C}$ ;  $^1\text{H}$  NMR (400MHz, DMSO- $d_6$ )  $\delta$  (ppm) 6.42 (s, 1 H, CH), 7.24-7.29 (m, 2 H,  $\text{ArH}_{2,6}$ ), 7.59-7.63 (m, 2 H,  $\text{ArH}_{3,5}$ ), 7.70 (d,  $J = 8.8$  Hz, 2 H,  $\text{ArH}_{2,6}$ ), 7.92 (d,  $J = 8.8$  Hz, 2 H,  $\text{ArH}_{3,5}$ ), 8.63 (d,  $J = 4.8$  Hz, 1 H, pyrimidine  $H_6$ ), 10.33 (s, 1 H, NH);  $^{13}\text{C}$  NMR (100MHz, DMSO- $d_6$ )  $\delta$  (ppm) 61.31, 102.71, 111.08, 115.53, 115.75, 118.46, 119.53, 130.34, 130.42, 132.98, 144.61, 159.20, 159.96, 167.60; IR (KBr,  $\text{cm}^{-1}$ ) 2220 (CN); MS (EI)  $m/z$  337 [M-H] $^{-}$ .

### 5.2.9. 4-((4-(chloro(4-chlorophenyl)methyl)pyrimidin-2-yl)amino)benzotrile (7i).

Yield 48%; brown solid; mp 156.3-156.7°C; <sup>1</sup>H NMR (400MHz, DMSO-*d*<sub>6</sub>) δ (ppm) 6.40 (s, 1 H, CH), 7.16 (d, *J* = 5.2 Hz, 1 H, pyrimidine *H*<sub>5</sub>), 7.47 (d, *J* = 8.4 Hz, 2 H, Ar*H*<sub>3,5</sub>), 7.56 (d, *J* = 8.4 Hz, 2 H, Ar*H*<sub>2,6</sub>), 7.68 (d, *J* = 8.8 Hz, 2 H, Ar*H*<sub>2,6</sub>), 7.90 (d, *J* = 8.8 Hz, 2 H, Ar*H*<sub>3,5</sub>), 8.61 (d, *J* = 5.2 Hz, 1 H, pyrimidine *H*<sub>6</sub>), 10.33 (s, 1 H, NH); <sup>13</sup>C NMR (100MHz, DMSO-*d*<sub>6</sub>) δ (ppm) 61.25, 102.74, 111.07, 118.45, 118.47, 128.73, 130.00, 132.91, 133.41, 137.92, 144.59, 159.18, 159.90, 167.41; IR (KBr, cm<sup>-1</sup>) 2215 (CN); MS (ESI) *m/z* 354 [M-H]<sup>-</sup>.

**5.2.10. 4-((4-(4-bromophenyl)chloromethyl)pyrimidin-2-yl)amino)benzonitrile (7j).**

Yield 55%; yellow solid; mp 194.5-195.3°C; <sup>1</sup>H NMR (400MHz, DMSO-*d*<sub>6</sub>) δ (ppm) 6.42 (s, 1 H, CH), 7.18 (d, *J* = 4.8 Hz, 1 H, pyrimidine *H*<sub>5</sub>), 7.51 (d, *J* = 8.0 Hz, 2 H, Ar*H*<sub>3,5</sub>), 7.63 (d, *J* = 8.0 Hz, 2 H, Ar*H*<sub>2,6</sub>), 7.69 (d, *J* = 8.4 Hz, 2 H, Ar*H*<sub>2,6</sub>), 7.89 (d, *J* = 8.4 Hz, 2 H, Ar*H*<sub>3,5</sub>), 8.62 (d, *J* = 5.2 Hz, 1 H, pyrimidine *H*<sub>6</sub>), 10.33 (s, 1 H, NH); <sup>13</sup>C NMR (100MHz, DMSO-*d*<sub>6</sub>) δ (ppm) 61.25, 102.71, 111.12, 118.45, 122.00, 130.30, 131.68, 132.94, 138.34, 144.58, 159.16, 159.96, 167.35; IR (KBr, cm<sup>-1</sup>) 2219 (CN); MS (ESI) *m/z* 417 [M+H<sub>2</sub>O]<sup>+</sup>.

**5.2.11. 4-((4-(chloro(naphthalen-1-yl)methyl)pyrimidin-2-yl)amino)benzonitrile (7k).**

Yield 55%; yellow solid; mp 174.8-175.3°C; <sup>1</sup>H NMR (400MHz, DMSO-*d*<sub>6</sub>) δ (ppm) 7.17 (s, 1 H, CH), 7.19 (d, *J* = 4.8 Hz, 1 H, pyrimidine *H*<sub>5</sub>), 7.25-8.16 (m, 11 H, Ar*H*<sub>4</sub>+Nap*H*<sub>7</sub>), 8.64 (d, *J* = 5.2 Hz, 1 H, pyrimidine *H*<sub>6</sub>), 10.30 (s, 1 H, NH); <sup>13</sup>C NMR (100MHz, DMSO-*d*<sub>6</sub>) δ (ppm) 59.79, 102.60, 111.34, 118.35, 123.72, 125.48, 126.11, 126.76, 127.34, 128.89, 129.48, 130.06, 132.81, 133.56, 134.64, 144.57, 159.06, 159.77, 168.01; IR (KBr, cm<sup>-1</sup>) 2215 (CN); MS (ESI) *m/z* 369 [M-H]<sup>-</sup>.

**5.2.12. 4-((4-(4-(tert-butyl)phenyl)chloromethyl)-6-methylpyrimidin-2-yl)amino)benzonitrile (7l).**

Yield 65%; ivory solid; mp 162.5-163.2°C; <sup>1</sup>H NMR (400MHz, DMSO-*d*<sub>6</sub>) δ (ppm) 1.23 (s, 9 H, *t*-butyl), 2.42 (s, 3 H, Me), 6.26 (s, 1 H, CH), 7.09 (s, 1 H, pyrimidine *H*<sub>5</sub>), 7.40 (d, *J* = 8.4 Hz, 2 H, Ar*H*<sub>2,6</sub>), 7.48 (d, *J* = 8.4 Hz, 2 H, Ar*H*<sub>3,5</sub>), 7.67 (d, *J* = 8.8 Hz, 2 H, Ar*H*<sub>2,6</sub>), 7.97 (d, *J* = 8.8 Hz, 2 H, Ar*H*<sub>3,5</sub>), 10.25 (s, 1 H, NH); <sup>13</sup>C NMR (100MHz, DMSO-*d*<sub>6</sub>) δ (ppm) 23.78, 30.95, 34.30, 62.28, 102.38, 110.32, 118.31, 125.40, 127.75, 132.86, 136.09, 144.84, 151.09, 158.99, 167.52, 169.47; IR (KBr, cm<sup>-1</sup>) 2216 (CN); MS (ESI) *m/z* 389 [M-H]<sup>-</sup>.

**5.2.13. 4-((4-(chloro(4-fluorophenyl)methyl)-6-methylpyrimidin-2-yl)amino)benzonitrile (7m).**

Yield 68%; light yellow solid; mp 127.8-128.2°C; <sup>1</sup>H NMR (400MHz, DMSO-*d*<sub>6</sub>) δ (ppm) 2.42 (s, 3H, Me), 6.35 (s, 1H, CH), 7.07 (s, 1 H, pyrimidine *H*<sub>5</sub>), 7.22-7.27 (m, 2 H, Ar*H*<sub>2,6</sub>), 7.59-7.62 (m, 2 H, Ar*H*<sub>3,5</sub>), 7.67 (d, *J* = 8.8 Hz, 2 H, Ar*H*<sub>2,6</sub>), 7.93 (d, *J* = 8.8 Hz, 2 H, Ar*H*<sub>3,5</sub>), 10.25 (s, 1 H, NH); <sup>13</sup>C NMR (100MHz, DMSO-*d*<sub>6</sub>) δ (ppm) 23.83, 61.49, 102.51, 110.45, 115.46, 115.67, 118.37, 119.60, 130.30, 130.39, 132.91, 135.40, 135.43, 159.07, 167.24, 169.73; IR (KBr, cm<sup>-1</sup>) 2213 (CN); MS (ESI) *m/z* 351 [M-H]<sup>-</sup>.

**5.2.14. 4-((4-(4-bromophenyl)chloromethyl)-6-methylpyrimidin-2-yl)amino)benzonitrile (7n).**

Yield 65%; light yellow solid; mp 169.3-169.6°C; <sup>1</sup>H NMR (400MHz, DMSO-*d*<sub>6</sub>) δ (ppm) 2.43 (s, 3 H, Me), 6.37 (s, 1 H, CH), 7.09 (s, 1 H, pyrimidine *H*<sub>5</sub>), 7.51 (d, *J* = 8.4 Hz, 2 H, Ar*H*<sub>2,6</sub>), 7.64 (d, *J* = 8.4 Hz, 2 H, Ar*H*<sub>3,5</sub>), 7.68 (d, *J* = 8.8 Hz, 2 H, Ar*H*<sub>2,6</sub>), 7.90 (d, *J* = 8.8 Hz, 2 H, Ar*H*<sub>3,5</sub>), 10.27 (s, 1 H, NH); <sup>13</sup>C NMR (100MHz, DMSO-*d*<sub>6</sub>) δ (ppm) 23.84, 61.36, 102.48, 110.54, 118.33, 121.93, 130.29, 131.64, 132.94, 138.49, 144.78,

159.02, 166.98, 169.79; IR (KBr, cm<sup>-1</sup>) 2212 (CN); MS (ESI) *m/z* 411 [M-H]<sup>-</sup>.

**5.2.15. 4-((4-((4-(tert-butyl)phenyl)chloromethyl)-5-methylpyrimidin-2-yl)amino)benzonitrile (7o).**

Yield 62%; brown solid; mp 119.3-120.0 °C <sup>1</sup>H NMR (400MHz, DMSO-*d*<sub>6</sub>) δ (ppm) 1.25 (s, 9 H, *t*-butyl), 2.23 (s, 3 H, Me), 6.55 (s, 1 H, CH), 7.43 (d, *J* = 8.4 Hz, 2 H, Ar*H*<sub>2,6</sub>), 7.51 (d, *J* = 8.4 Hz, 2 H, Ar*H*<sub>3,5</sub>), 7.67 (d, *J* = 8.4 Hz, 2 H, Ar*H*<sub>2,6</sub>), 7.95 (d, *J* = 8.8 Hz, 2 H, Ar*H*<sub>3,5</sub>), 8.41 (s, 1 H, pyrimidine *H*<sub>6</sub>), 10.21 (s, 1 H, NH); <sup>13</sup>C NMR (100MHz, DMSO-*d*<sub>6</sub>) δ (ppm) 14.04, 31.03, 34.38, 59.43, 102.04, 118.04, 119.39, 125.37, 128.10, 132.93, 134.98, 145.00, 151.07, 157.90, 160.28, 164.47; IR (KBr, cm<sup>-1</sup>) 2210 (CN); MS (ESI) *m/z* 389 [M-H]<sup>-</sup>.

**5.2.16. 4-((4-(chloro(4-fluorophenyl)methyl)-5-methylpyrimidin-2-yl)amino)benzonitrile (7p).**

Yield 52%; ivory solid; mp 159.7-160.3 °C; <sup>1</sup>H NMR (400MHz, DMSO-*d*<sub>6</sub>) δ (ppm) 2.25 (s, 3 H, Me), 6.63 (s, 1 H, CH), 7.26-7.30 (m, 2 H, Ar*H*<sub>2,6</sub>), 7.62-7.67 (m, 4 H, Ar*H*<sub>3,5</sub> + Ar*H*<sub>2,6</sub>), 7.88 (d, *J* = 8.4 Hz, 2H, Ar*H*<sub>3,5</sub>), 8.43 (s, 1 H, pyrimidine *H*<sub>6</sub>), 10.19 (s, 1 H, NH); <sup>13</sup>C NMR (100MHz, DMSO-*d*<sub>6</sub>) δ (ppm) 13.97, 58.69, 102.13, 115.31, 115.53, 117.99, 119.58, 119.62, 130.60, 130.68, 132.91, 134.22, 144.91, 157.85, 160.45, 164.21; IR (KBr, cm<sup>-1</sup>) 2216 (CN); MS (ESI) *m/z* 351 [M-H]<sup>-</sup>.

**5.2.17. 4-((4-(1-(4-(tert-butyl)phenyl)-1-hydroxyethyl)-5-methylpyrimidin-2-yl)amino)benzonitrile (7q).**

Yield 45%; ivory solid; mp 202.8-203.3°C; <sup>1</sup>H NMR (400MHz, DMSO-*d*<sub>6</sub>) δ (ppm) 2.26 (s, 3 H, Me), 6.62 (s, 1 H, CH), 7.53 (d, *J* = 8.4 Hz, 2 H, Ar*H*<sub>2,6</sub>), 7.62-7.66 (m, 4 H, Ar*H*<sub>3,5</sub> + Ar*H*<sub>2,6</sub>), 7.81 (d, *J* = 8.8 Hz, 2 H, Ar*H*<sub>3,5</sub>), 7.43 (s, 1 H, pyrimidine *H*<sub>6</sub>), 10.17 (s, 1 H, NH); <sup>13</sup>C NMR (100MHz, DMSO-*d*<sub>6</sub>) δ (ppm) 13.96, 58.74, 102.11, 117.96, 119.75, 121.80, 130.55, 131.43, 132.82, 137.36, 144.85, 157.76, 160.48, 164.03; IR (KBr, cm<sup>-1</sup>) 2216 (CN); MS (ESI) *m/z* 411 [M-H]<sup>-</sup>.

**5.3.1. 4-((4-(bromo(phenyl)methyl)pyrimidin-2-yl)amino)benzonitrile (7r).**

Yield 72%; yellow solid; mp 120.2-121.0°C; <sup>1</sup>H NMR(400MHz, DMSO-*d*<sub>6</sub>) δ (ppm) 6.42 (s, 1 H, CH), 7.11 (d, *J* = 4.8 Hz, 1 H, pyrimidine *H*<sub>5</sub>), 7.20 (d, *J* = 8.0 Hz, 2 H, Ar*H*<sub>2,6</sub>), 7.51 (d, *J* = 8.0 Hz, 2 H, Ar*H*<sub>3,5</sub>), 7.71 (d, *J* = 8.8 Hz, 2 H, Ar*H*<sub>2,6</sub>), 7.98 (d, *J* = 8.8 Hz, 2 H, Ar*H*<sub>3,5</sub>), 8.58 (d, *J* = 5.2 Hz, 1 H, pyrimidine *H*<sub>6</sub>), 10.32 (s, 1 H, NH); <sup>13</sup>C NMR (100MHz, DMSO-*d*<sub>6</sub>) δ (ppm) 61.17, 102.70, 111.11, 118.44, 118.49, 128.74, 130.00, 132.93, 133.35, 137.92, 144.57, 159.16, 159.96, 167.38; IR (KBr, cm<sup>-1</sup>) 2219 (CN); MS (ESI) *m/z* 363 [M-H]<sup>-</sup>.

**5.3.2. 4-((4-(bromo(*p*-tolyl)methyl)pyrimidin-2-yl)amino)benzonitrile (7s).**

Yield 70%; light yellow solid; mp 161.7-162.4°C; <sup>1</sup>H NMR(400MHz, DMSO-*d*<sub>6</sub>) δ (ppm) 2.28 (s, 3 H, Me), 6.42 (s, 1 H, CH), 7.12 (d, *J* = 4.8 Hz, 1 H, pyrimidine *H*<sub>5</sub>), 7.20 (d, *J* = 8.0 Hz, 2 H, Ar*H*<sub>2,6</sub>), 7.51 (d, *J* = 8.0 Hz, 2 H, Ar*H*<sub>3,5</sub>), 7.71 (d, *J* = 8.8 Hz, 2 H, Ar*H*<sub>2,6</sub>), 7.98 (d, *J* = 8.8 Hz, 2 H, Ar*H*<sub>3,5</sub>), 8.58 (d, *J* = 5.2 Hz, 1 H, pyrimidine *H*<sub>6</sub>), 10.32 (s, 1 H, NH); <sup>13</sup>C NMR (100MHz, DMSO-*d*<sub>6</sub>) δ (ppm) 20.71, 53.01, 102.67, 111.50, 118.49, 128.69, 129.19, 132.96, 135.79, 138.22, 144.66, 159.24, 159.78, 167.85; IR (KBr, cm<sup>-1</sup>) 2220 (CN); MS (ESI) *m/z* 377 [M-H]<sup>-</sup>.

**5.4. Anti-HIV activity assay**

The anti-HIV activity and cytotoxicity of the compounds **7a-s** were evaluated against wild type HIV-1 strain IIIIB, a double RT

mutant (K103N + Y181C) HIV-1 strain and HIV-2 strain ROD in MT-4 cell cultures using the 3-(4, 5-dimethylthiazol-2-yl)-2,5-diphenyltetrazoliumbromide (MTT) method.<sup>17,18</sup> Briefly, stock solutions (10 × final concentration) of test compounds were added in 25 µl volumes to two series of triplicate wells so as to allow simultaneous evaluation of their effects on mock-and HIV-infected cells at the beginning of each experiment. Serial 5-fold dilutions of test compounds were made directly in flat-bottomed 96-well microtiter trays using a Biomek 3000 robot (Beckman instruments). Untreated control HIV-1 and mock-infected cell samples were included for each sample. Virus stock (50 µl) at 100-300 CCID<sub>50</sub> (50% cell culture infectious dose) or culture medium was added to either the virus-infected or mock-infected cells of the microtiter tray. Mock-infected cells were used to evaluate the effect of test compounds on uninfected cells in order to assess the cytotoxicity of the test compounds. Exponentially growing MT-4 cells were centrifuged for 5 min at 220 g and the supernatant was discarded. The MT-4 cells were resuspended at 6 × 10 cells/ml and 50 µL volumes were transferred to the microtiter tray wells. Five days after infection, the viability of mock-and HIV-infected cells was examined spectrophotometrically by the MTT assay.

The MTT assay is based on the reduction of yellow colored MTT (Acros Organics) by mitochondrial dehydrogenase activity of metabolically active cells to a blue-purple formazan that can be measured spectrophotometrically. The absorbances were read in an eight-channel computer-controlled photometer (Infinite M1000, Tecan) at two wavelengths (540 and 690 nm). All data were calculated using the median OD (optical density) values of tree wells. The 50% cytotoxic concentration (CC<sub>50</sub>) was defined as the concentration of the test compounds that reduced the absorbance (OD<sub>540</sub>) of the mock-infected control sample by 50%. The concentration achieving 50% protection from the cytopathic effect of the virus in infected cells was defined as the 50% effective concentration (EC<sub>50</sub>).

### 5.5. Molecular simulation

### Acknowledgments

This research was financially supported by grants from Chinese National Science and Technology Major Project (No. 2012ZX09103101-068), National Natural Science Foundation of China (No. 81172918), Shanghai Municipal Natural Science Foundation (No.13ZR1402200) and KU Leuven (GOA 10/014).

### References and notes

- Mehellou, Y.; De Clercq, E.; *J. Med. Chem.*, **2010**, *53*, 521.
- Chen, X.; Zhan, P.; Li, D.; De Clercq, E.; Liu, X.; *Curr. Med. Chem.*, **2011**, *18*, 359.
- De Béthune, M.P.; *Antiviral. Res.*, **2010**, *85*, 75.
- Li, D. Y.; Zhan, P.; De Clercq, E.; Liu, X.Y. *J Med Chem.*, **2012**, *55*, 3595-3613.
- Zhang, L.; Zhan, P.; Chen, X.; Li, Z.; Xie, Z.; Zhao, T.; Liu, H.; De Clercq, E.; Pannecouque, C.; Balzarini, J.; Liu, X.; *Bioorg. Med. Chem.*, **2014**, *22*, 633-642.
- Yang, S.; Pannecouque, C.; Daelemans, D. Ma, X. Liu, Y.; Chen, F.E.; De Clercq, E.; *Eur. J. Med. Chem.*, **2013**, *65*, 134-14.
- Chen, X.; Liu, X.; Meng, Q.; Wang, D.; Liu, H.; De Clercq, E.; Pannecouque, C.; Balzarini, J.; Liu, X.; *Bioorg. Med. Chem. Lett.*, **2013**, *24*, 6593-6597.
- Chen, X.; Li, Y.; Ding, S.; Balzarini, J.; Pannecouque, C.; De Clercq, E.; Liu, H.; Liu, X.; *Chem. Med. Chem.*, **2013**, *7*, 1117-1126.
- Bailey, C. M.; Sullivan, T. J.; Iyidogan, P.; Tirado-Rives, J.; Chung, R.; Ruiz-Caro, J.; Mohamed, E.; Jorgensen, W.; Hunter, R.; Anderson, K. S.; *J. Med. Chem.*, **2013**, *10*, 3889-3903.
- Gu, S. X.; He, Q. Q.; Yang, S. Q.; Ma, X. D.; Chen, F. E.; De Clercq, E.; Balzarini, J.; Pannecouque, C. *Bioorg Med Chem.*, **2011**, *19*, 5117-5124.
- Erdelyi, M.; *Chem. Soc. Rev.* **2012**, *41*, 3547-3557.
- Metrangolo, P.; Meyer, F.; Pilati, T.; Resnati, G.; Terraneo, G.; *Angew. Chem., Int. Ed. Engl.* **2008**, *47*, 6114-6127.
- Xu, Z.; Yang, Z.; Liu, Y.; Lu, Y.; Chen, K.; Zhu, W.; *J. Chem. Inf. Model.*, **2014**, doi.org/10.1021/ci400539q.
- Lu, Y.; Shi, T.; Wang, Y.; Yang, H.; Yan, X.; Luo, X.; Jiang, H.; Zhu, W. *J. Med. Chem.*, **2009**, *52*, 2854-2862.
- Lu, Y.; Wang, Y.; Zhu, W.; *Phys. Chem. Chem. Phys.* **2010**, *12*, 4543-4551.
- Bondi, A.; *J. Phys. Chem.* **1964**, *68*, 441-451
- Pannecouque, C.; Daelemans, D.; De Clercq, E. *Nat Protoc.*, **2008**, *3*, 427-434.
- Pauwels, R.; Balzarini, J.; Baba, M.; Snoeck, R.; Schols, D.; Herdewijn, P.; Desmyter, J.; De Clercq, E. *J Virol Methods.*, **1988**, *20*, 309-321.

Molecular modeling was carried out with the Tripos molecular modeling packages Sybyl-1.2. All the molecules for docking were built using standard bond lengths and angles from Sybyl-1.2/base Builder and then optimized using the Tripos force field for 1000 generations two times or more, with an energy gradient of 0.001 kcal/(molÅ) and Gasteiger-Hückel charges loaded, until the minimized conformers of the ligand were the same. The X-ray co-crystal structure of wild type RT in complex with ETV in the Brookhaven Protein Data Bank (PDB entry code: 3MEC) was used for docking. Prior to docking, the protein receptor was preprocessed by removing the initial ligand. Then the free protein was prepared by removing water molecules and other unnecessary small molecules, and adding hydrogen atoms. The atomic charges were recalculated using the Kollman all-atom approach for the protein and the Gasteiger-Hückel approach for the ligand. The geometry of the non-nucleoside binding site (NNIBP) was defined by selecting all the residues within of the initial inhibitor. Surflex-Dock default settings were used for other parameters, such as the number of starting conformations per molecule (set to 0), the size to expand search grid (set to 8Å), the maximum number of rotatable bonds per molecule (set to 100), and the maximum number of poses per ligand (set to 20). During the docking procedure, all of the single bonds in residue side chains inside the defined RT binding pocket were regarded as rotatable or flexible, and the ligand was allowed to rotate on all single bonds and move flexibly within the tentative binding pocket. The binding interaction energy was calculated to include van der Waals, electrostatic and torsional energy terms defined in the Tripos force field. The structure optimization was performed for 20000 generations using a genetic algorithm, and the 20 best scoring ligand-protein complexes were kept for further analyses. The -log(Kd)<sup>2</sup> values of the 20 best scoring complexes, which represented the binding affinities of ligand with RT, ranged over a wide scope of functional classes. Therefore, only the highest scoring 3D structural model of the ligand-bound RT was chosen to define the binding interaction.

Click here to remove instruction text...